DEVELOPMENT OF A PHOSWICH DETECTOR SYSTEM FOR RADIOXENON MONITORING

W. Hennig[1], W.K. Warburton[1], A. Fallu-Labruyere[1], K. Sabourov[1], M.W. Cooper[2], J.I. McIntyre[2], A. Gleyzer[3], M. Bean[4], E. P. Korpach[5], K. Ungar[5], W. Zhang[5], P. Mekarski[5]

[1]XIA LLC, 31057 Genstar Rd, Hayward, CA 94544, USA
[2]Pacific Northwest National Laboratory, Richland, WA 99352, USA
[3]PhotoPeak, Inc, 10180 Queens Way # 3-5 Chagrin Falls, Ohio 44023, USA
[4]Radiation Protection Bureau, Health Canada, Ottawa, Ontario K1A 1C1, Canada

Abstract

Measurement of radioactive xenon in the atmosphere is one of several techniques to detect nuclear weapons testing. For high sensitivity, some existing systems use beta/gamma coincidence detection to suppress background, which is very effective, but increases complexity due to separate beta and gamma detectors that require careful calibration and gain matching. In this paper, we will describe the development and evaluation of a simpler detector system, named PhosWatch, consisting of a CsI(Tl)/BC-404 phoswich well detector, digital readout electronics, and pulse shape analysis algorithms implemented in a digital signal processor on the electronics, and compare its performance to existing multi-detector systems.

Introduction

Systems to measure the amount of radioactive xenon in the atmosphere, part of the International Monitoring System established by the Comprehensive Nuclear-Test-Ban Treaty to detect nuclear weapons testing, have been installed in several locations around the world. Several of these radioxenon detection systems, e.g. the Automated Radioxenon Sampler and Analyzer[1] (ARSA) or the Swedish Automatic Unit for Noble gas Acquisition[2] (SAUNA), use beta/gamma coincidence detection to suppress non-coincident background and achieve high sensitivity to the coincidence events characteristic of the radioxenon isotopes of interest.

While these systems are very sensitive to small amounts of radioxenon, their complex arrangement of separate beta and gamma detectors also requires careful calibration and gain matching, which can make them cumbersome to operate. An alternative approach is the use of a single phoswich detector[3,4,5] in which beta/gamma coincidences are detected by pulse shape analysis (PSA). The objective of the work presented here was to develop a radioxenon detector system that can be used as a drop-in replacement for ARSA or SAUNA detector units. This system, named PhosWatch, consists of a CsI(Tl)/BC-404 phoswich well detector, digital readout electronics, and PSA functions implemented on-board the electronics. In the following, we will describe the development of the system, characterize the performance of the phoswich detectors, and present initial results from a side-by-side evaluation of the PhosWatch system with existing radioxenon detector systems.

Experimental

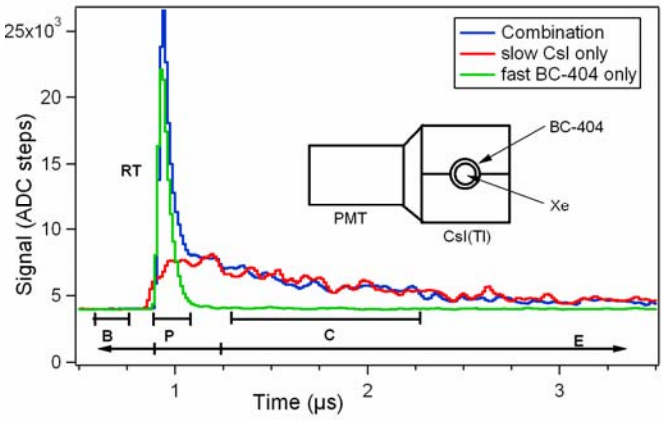

Figure 1: Waveforms from phoswich well detector. The pulse shape analysis uses sums B, P and C and rise time RT, as well as a weighted integral E extending over a larger area to distinguish fast, slow and fast/slow pulses and compute the fraction of energy deposited in each scintillator.

Having previously built two prototypes to determine the best geometry for manufacturing and light collection[6], we built a total of 7 phoswich well detectors in a small-scale production, named PW3a-PW9. They all consist of a 1"-diameter BC-404 plastic cell with 2 mm wall thickness enclosed in, and optically coupled to, a 3" diameter, 3" tall CsI(Tl) cylinder. The fast plastic scintillator cell contains the Xe gas and by geometry mainly absorbs beta particles and conversion electrons, the slower CsI scintillator mainly absorbs X-rays and gamma rays. Beta/gamma coincidences create characteristic "fast/slow" signals (Figure 1) that can easily be distinguished from "slow only" or "fast only" non-coincident interactions by PSA algorithms described previously[4]. PW4, PW5, and PW8 were read out by PMT model 9305KB (ET Enterprises); PW3a, PW6, PW7, and PW9 use PMT model R1307 (Hamamatsu). (PW3a is the second prototype PW3 rebuilt with a new PMT and crystal.) Detectors were tested for vacuum tightness and typically leaked less than 1 Torr/h when evacuated to 1 Torr and disconnected from the pump.

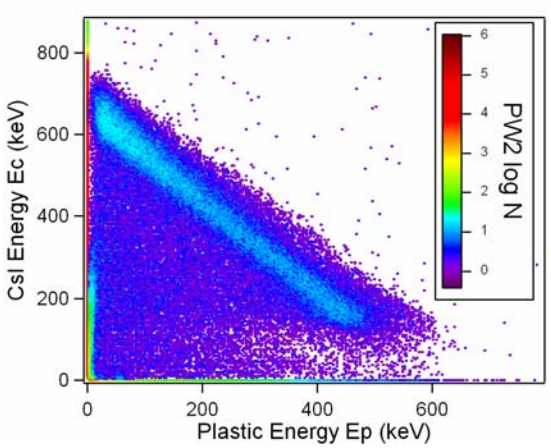

Figure 2: 2D histogram from phoswich detector with ^{137}Cs source. Non-coincident events are contracted to the axes.

The PMT signal was connected to a DGF Pixie-4 module[7]. The Pixie-4 has an on-board digital signal processor (DSP) that in standard operation computes pulse heights, records time stamps, and accumulates MCA spectra in on-board memory. For the phoswich application, the DSP was programmed to also compute the PSA sums and rise time indicated in Figure 1, categorize events as CsI only, BC-404 only or combination of both, compute the energy deposited in the CsI (Ec) and the BC-404 (Ep), and bin the result into 1D and 2D spectra. A typical 2D spectrum with a ^{137}Cs source is shown in Figure 2. In the simplest mode of operation, it is only necessary to start and stop data acquisition in the Pixie-4 according to the sample preparation schedule, and read out the Pixie-4 memory to retrieve spectrum data for isotope analysis routines. For more control and flexibility, list mode data containing energies and PSA results can be read as well and can be used to re-compute energies and/or re-bin spectra with custom binning parameters at a later time. Since Ec and Ep are determined from measurements in a single channel, their relative energy scale is fixed (a detector constant derived from the relative light output of the scintillators). This means that in Figure 2 changes in PMT gain will move the 662 keV peak on the Ec axis and the intersect of the line of constant energy with the Ep axis, but the slope of the line will remain constant. Thus gain calibration is much simpler than in systems with separate beta and gamma detectors.

Results and Discussion

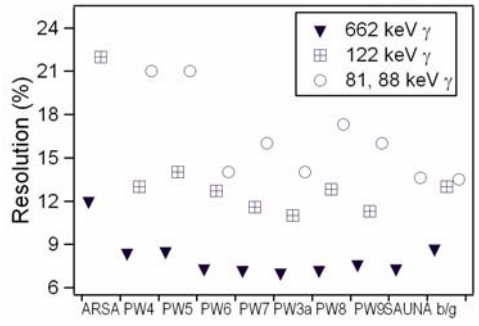

Figure 3: Resolution of photon energy for radioxenon detectors. Phoswich detectors are listed in order of production. The 80/88 keV data used internal ^{109}Cd or ^{133}Xe sources, other data used ^{137}Cs and ^{57}Co sources outside the detector. Non-phoswich data are from measurements at HealthCanada or literature[8,9,10].

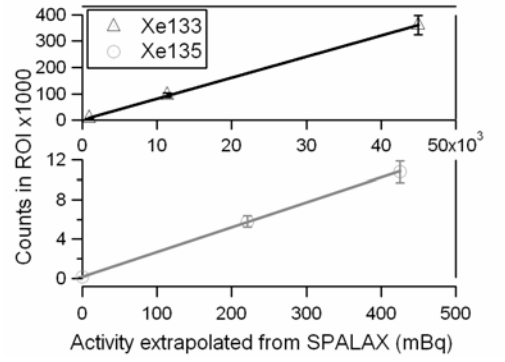

Figure 4: Counts in PW5 region of interest vs. nominal activity from SPALAX measurement for several samples from a Canadian monitoring

Detectors were characterized by measuring resolutions at various energies with a number of test sources. As shown in Figure 3, the photon energy resolutions of PW3a-PW9 at medium to high energy are significantly better than resolutions reported for the ARSA detector[8], and the later detectors (PW6-PW9), with improvements in detector assembly and careful selection of PMTs for low noise, reach an average ~7.3% FWHM at 662 keV. These later detectors thus match or exceed the resolutions obtained with Pacific Northwest National Laboratory's redesigned beta/gamma detector[9] in the preferred CsI(Na) variant and a SAUNA II detector[10]. At low photon energy (30 keV), the phoswich detectors typically obtain 28-35% compared to ~32% for ARSA, 23-30% for SAUNA, and ~18% for the redesigned beta/gamma detector. For 129 keV conversion electrons the phoswich resolution is typically 26-33%, compared to 25-30% for ARSA, 19% for SAUNA and ~25% for the redesigned beta/gamma detector. Note that count rates and other experimental conditions can not be assumed to be the same for measurements performed at different times and institutions.

In monitoring applications, the samples of radioxenon collected are very small, so the background count rate of the detector has to be as low as possible. In a lead enclosure (2" lead with 0.5" copper lining) we measure an overall rate of 3–8 counts/s for PW4–5 and PW8-9, of which ~0.02–0.08 counts/s are coincidences, and only ~0.002-0.004 counts/s fall in the ^{133}Xe regions of interest (ROI) at 30 keV and 80 keV. PW6, PW7, and PW3a showed higher background rates (~10 counts/s total, ~0.5 counts/s coincident) due to small amounts of ^{40}K in the PMT and the CsI. This contamination has been eliminated for PW8 and PW9 by careful screening of crystals and PMTs before assembly. All detectors reject over 99% of radiation from an external ^{137}Cs

source as non-coincident. In comparison, the background rate is about 30 counts/s in the larger ARSA detector (~0.1 counts/s coincident), and about 7.5-12 counts/s in the similar sized SAUNA detector[10] (0.02-0.03 counts/s coincident).

As part of the evaluation of the PhosWatch system in monitoring application, Xe samples acquired with a SPALAX system[11] were re-measured in parallel with PW5 and a SAUNA system at Health Canada. Figure 4 shows the number of coincidence events detected by PW5 in ROIs at Ec = 80 keV and Ec = 250 keV as a function of ^{133}Xe and ^{135}Xe activity measured by the SPALAX system. While error bars must be assumed to be 10% or more due to uncertainties in the sample transfer, disregard of other isotopes, and simplifications in the correction for decay between measurements, the data shows a good linear correlation, indicating that PW5 results are consistent with the SPALAX results.

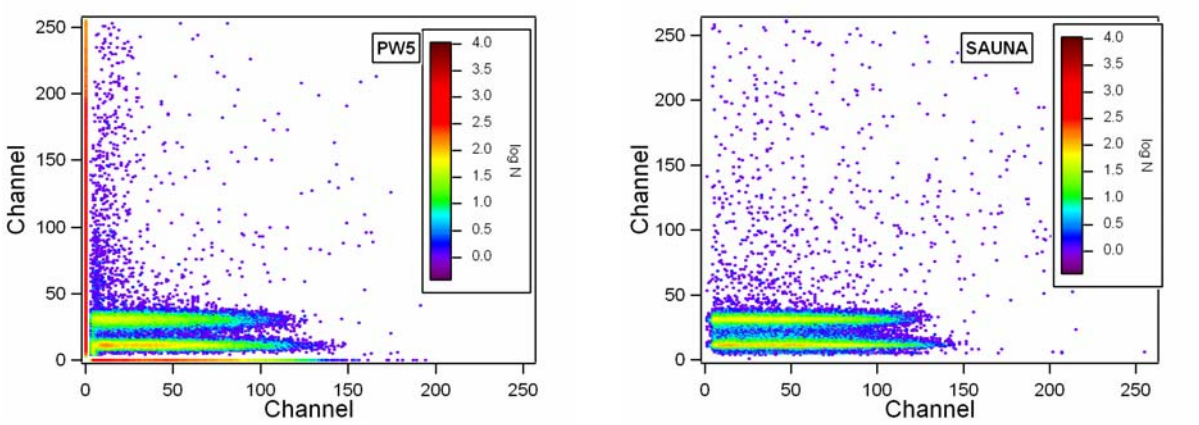

Figure 5: 2D histograms from a SPALAX sample split between PW5 (left) and SAUNA (right).

Figures 5 and 6 show 2D and 1D energy spectra for a SPALAX sample divided between PW5 and a SAUNA. At the low photon energies of this sample, peak resolution is better for this SAUNA than for PW5 (the latter being one of our earlier phoswich detectors) but since the quantitative analysis only uses the number of counts in a ROI and peaks are well separated, the difference is not critical. In this and other measurements, we also observe that the background in PW5 is lower, and that the "memory effect" from Xe retained in the plastic from previous samples is about equal in this SAUNA and in PW5.

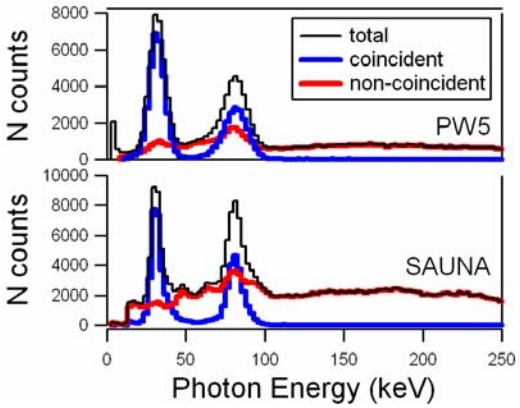

Figure 6: 1D spectra of photon energy for PW5 and SAUNA (data from Figure 5 projected to vertical axis).

To obtain a basis for quantitative analysis of PhosWatch spectra, the detector geometry was modeled with a Geant4 simulation, both for radiation processes and optical processes. We assumed the BC-404 cell to be filled with 15% xenon and 85% nitrogen, and used the following input parameters (besides literature constants): an outer reflectivity of 0.95, PMT quantum efficiency 30%, photocathode reflectivity 17%, signal risetimes (after a low pass Nyquist filter in the electronics) 100 ns for CsI, 13 ns for BC-404, and a coincidence time window for the PSA of 100 ns. We then compute the coincidence detection efficiency for each ROI as

$$\varepsilon_{\beta\gamma\_ROI} = \frac{C_{ROI}}{C_A \times BR_{ROI}}, \qquad (1)$$

where C_{ROI} and C_A are the number of counts in the ROI and in total, respectively, and BR_{ROI} is the beta-gamma branching ratio for the ROI. To verify the simulation, we used the data in Figure 5 and a preceding background measurement to compute $\varepsilon_{\beta\gamma\_133Xe\_30}$ and $\varepsilon_{\beta\gamma\_133Xe\_80}$ from the product of gamma and beta efficiency, which are obtained from the ratios of coincident counts (in the ROI) and singles counts (projection of coincident and non-coincident events to beta or gamma axis). As shown in Figure 7, the simulated $\varepsilon_{\beta\gamma\_ROI}$ (x marks) agree well with the $\varepsilon_{\beta\gamma\_ROI}$ estimated from the data (solid circles). Also shown are $\varepsilon_{\beta\gamma\_ROI}$ given by the manufacturer for the SAUNA system at Health Canada (solid squares) and phoswich $\varepsilon_{\beta\gamma\_ROI}$ derived from Xe and Rn measurements at PNNL, using 98% detection efficiency for conversion electrons from ^{131m}Xe as the starting point[12] (open symbols). Note that again experimental conditions and especially ROI boundaries may vary. In particular, in PNNL measurements, the Rn count rate was very low and backgrounds were high, leading to large

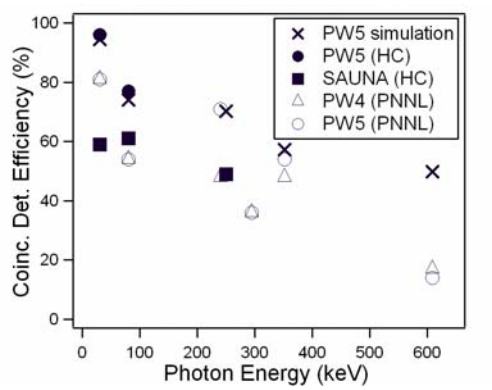

Figure 7: Coincidence detection efficiency of PW4, PW5 and a SAUNA detector installed at Health Canada

uncertaincies in the computed efficiency, which may explain the difference to the simulation. The most directly comparable efficiency between the different systems and methods may thus be $\varepsilon_{\beta\gamma\_131mXe}$, because with the clearly defined peak well away from the axes, the effects of ROI boundaries are minimal. This value is 79.8% from simulations, 81% from the PNNL measurements, and 57% for this SAUNA. Overall, we see that $\varepsilon_{\beta\gamma\_ROI}$ is significantly higher for PW5 than for this SAUNA, especially at low energy. One reason for the higher efficiency in the phoswich is that detection of low-energy X-rays is enhanced if they are in coincidence with a beta particle since the latter creates a large pulse in the PMT that is easy to trigger on.

Using the simulated $\varepsilon_{\beta\gamma\_ROI}$ and a preceding background measurement for quantitative analysis of the PW5 data shown in Figure 5, we compute the concentration of ^{133}Xe in the original sample to be 127 mBq/m^3. Concentrations for other isotopes were below 20 mBq/m^3. Computing the PW5 ^{133}Xe concentration separately for 6 ROIs that contain ^{133}Xe contributions showed variations from 122-129 mBq/m^3, indicating very good consistency within the PW5 measurement itself. The minimum detectable concentration (MDC) for this data is 0.49 mBq/m^3. Analysis of the SAUNA data taken in parallel to the PW5 measurement computed a ^{133}Xe concentration of 155 mBq/m^3 with an MDC of 0.21 mBq/m^3. Variations in different ROIs ranged from 145-168 mBq/m^3, about twice the fluctuations than in PW5. The original SPALAX analysis measured a concentration of 194 mBq/m^3. (It has no comparable ROIs since it is not a beta/gamma coincidence system). In a second data set, PW5 measured a ^{133}Xe concentration of 1274 mBq/m^3 (ROI variation 1208-1288 mBq/m^3), the SAUNA measured 1486 mBq/m^3 (1380-1691 mBq/m^3), and the SPALAX system measured 1873 mBq/m^3. We note that in both data sets, PW5 and SAUNA consistently measure ~65% and ~80% of the SPALAX values, respectively, and attribute this to the loss of sample volume during transfer and/or in the dead volume of the gas connections.

Conclusion

In summary, we developed a radioxenon detector unit, named "PhosWatch", consisting of a phoswich detector, readout electronics, and PSA functions to detect beta/gamma coincidences implemented on-board the electronics. Overall, PhosWatch energy resolutions are comparable to existing systems, matching or exceeding resolutions at mid-high energies (~7.3% FWHM for662 keV gamma rays for the later production batches) and reaching approximately 30% for both 30 keV energy X-rays and 129 keV conversion electrons. Background rates, memory effect, MDC, and coincidence detection efficiencies for the phoswich detectors are comparable to, and sometimes better than, values for existing systems. Evaluation of PW5 showed good consistency and precision in radioxenon detection tests with samples from monitoring systems. Requiring only a single PMT and electronics readout channel, the key benefit of the PhosWatch is its simpler setup, gain calibration and operation compared to the existing coincidence detection systems. In future work, we will continue the side-by-side evaluation, and explore performance improvements with electronics digitizing at 500 MHz (now under development), which should allow even better detection of coincidences since fast plastic pulses are better resolved.

ACKNOWLEDGEMENTS

This work was supported by the US Department of Energy under Award No. DE-FG02-04ER84121

REFERENCES

1. P.L. REEDER, T.W. BOWYER, R.W. PERKINS, J. Radioanal. Nuclear Chem. 235 (1998) p89.
2. A. RINGBOM, T. LARSON, A. AXELSON, K. ELMGREN, C. JOHANSSON, NIM A 508 (2003) p542.
3. J. H. ELY, C.E. AALSETH, J.I. McIntyre, J. Radioanal. Nuclear Chem. 263 No. 1 (2005) p245.
4. W. HENNIG, H. TAN, W.K. WARBURTON, J.I. McIntyre, IEEE TNS 53 Vol. 2 (2006) p620.
5. A.T. FARSONI, D.M. HAMBY, NIM A 578 (2007) p528.
6. W. HENNIG, H. TAN, A. FALLU-LABRUYERE, W.K. WARBURTON, J.I. McIntyre, A. GLEYZER, NIM A 579 (2007) 431.
7. W. HENNIG, Y.X. CHU, H. TAN, A. FALLU-LABRUYERE, W. K. WARBURTON, R. GRZYWACZ . NIM B 263 (2007) 175.
8. REEDER, P. L., T. W. BOWYER, J. I. McIntyre, W. K. PITTS, A. RINGBOM, C. JOHANSSON, NIM A 521 (2004) p586.
9. M.W. COOPER, J.I. McIntyre, T.W. BOWYER, A.J. CARMAN, J.C. HAYES, T.R. HEIMBIGNER, C.W. HUBBARD, L. LIDEY, K.E. LITKE, S.J. MORRIS, M.D. RIPPLINGER, R. SUAREZ, R. THOMPSON NIM A 579 (2007) p426.
10. A. RINGBOM, private communication, 2007.
11. J.-P. FONTAINE, F. POINTURIER, X. BLANCHARD, T. TAFFARY (2004). J. of Environmental Radioactivity 72 (2004) p129.
12. M.W. COOPER, J.C. HAYES, T.R. HEIMBIGNER, C.W. HUBBARD, J.I. McIntyre, M.D. RIPPLINGER, B.T. SCHROM, Proc. of the 29th Monitoring Research Review, LA-UR-07-5613, (2007) Vol. 2, p739.